

# Hydrothermal alteration mapping using ASTER data in Baogutu porphyry deposit, China

Q Li<sup>1,2</sup>, B Zhang<sup>1</sup>, L Lu<sup>1</sup> and Q Lin<sup>1</sup>

<sup>1</sup>Key Laboratory of Digital Earth Science, Institute of Remote Sensing and Digital Earth, Chinese Academy of Sciences

E-mail: qtli@ceode.ac.cn

**Abstract.** Remote sensing plays an important role in mineral exploration. One of its proven applications is extracting host-rock lithology and alteration zones that are related to porphyry copper deposits. An Advanced Spaceborne Thermal Emission and Reflection Radiometer (ASTER) was used to map the Baogutu porphyry deposit alteration area. A circular alteration mineral zoning pattern was clearly observed in the classification result of potassic, phyllic, argillic, propylitic zones. The potassic is characterized by biotite and anhydrite with an absorption feature centered at 1.94 and 2.1 $\mu$ m. The phyllic zone is characterized by illite and sericite that indicates an intense Al-OH absorption feature centered at 2.20 $\mu$ m. The narrower argillic zone including kaolinite and alunite displays a secondary Al-OH absorption feature at 2.17  $\mu$ m. The mineral assemblages of the outer propylitic zone are epidote, chlorite and calcite that exhibit absorption features at 2.335 $\mu$ m. The performance of Principal Component Analysis (PCA), Minimum Noise Fraction (MNF), band ratio (BR) and Constrained Energy Minimization (CEM) has been evaluated. These techniques identified new prospects of porphyry copper mineralization in the study areas. These results indicate that ASTER is a powerful tool in the initial steps of mineral exploration.

## 1. Introduction

Remote sensing instruments provide an opportunity to improve initial steps of ore deposits exploration as which providing detailed information on the mineralogy and rock types [1-7]. The porphyry ore deposits were generated by hydrothermal fluid processes which alter the mineralogy and chemical composition of the country rocks [8]. The altered rocks have diagnostic spectral absorption features due to its mineral assemblages [9]. Remote sensing technology has been used to detect hydrothermal alteration mineral assemblages for reconnaissance stages of porphyry copper and gold exploration [6, 10-12]. In the past 20 years, new spaceborne multispectral and hyperspectral remote sensing instruments have provided higher spectral resolution data that can be used for mineral exploration [8]. As well, the availability of laboratory-measured spectral data for rocks and minerals allows geologists to identify unique lithologies. Remote sensing technology is becoming an increasingly important tool for mineral exploration. The Advanced Spaceborne Thermal Emission and Reflection Radiometer (ASTER) is a multispectral imager that was launched on board NASA's Terra spacecraft in December, 1999 which covers the visible, near infrared (VNIR), short wave infrared (SWIR), and thermal infrared (TIR) spectral regions with 14 channels with high spatial, spectral and radiometric resolution [13]. ASTER sensor allows the discrimination and identification of

<sup>2</sup> To whom any correspondence should be addressed.



hydrothermal alteration minerals in the SWIR region. The ASTER bands in the SWIR were specifically selected to highlight the presence of spectral absorption features of minerals, such as clay, carbonates, sulfates and other hydrous phases due to overtones and combination tones of fundamental absorptions of Al-O-H, Mg-O-H, Si-O-H, and  $\text{CO}_3^{2-}$  [14,15]. The object of the study was to use ASTER data to map the hydrothermal alteration mineral zones associated with porphyry copper mineralization in Baogutu porphyry Cu–Mo deposit. The major part of this belt has well-exposed and sparse vegetated surface which is ideal for remote sensing investigations. The lithologic information and alteration zones associated with porphyry copper mineralization was extracted by the methods of Minimum Noise Fraction (MNF), Principal Component Analysis (PCA), band ratio and specialized Constrained Energy Minimization (CEM).

## 2. Geology of the study area

The Baogutu porphyry Cu–Mo deposit in Toli County is the largest porphyry copper deposit in the Junggar region of Xinjiang [16] locating at the southern side of the Dalabute fault in the West Junggar and tectonically along the margin of the Devonian–Carboniferous Dalabute–Kalamaili remnant ocean basin [17]. There are Lower Carboniferous Xibeikulasi, Baogutu, and Tailegula Formations which exposed in the Baogutu ore district. The Xibeikulasi Formation consists of a suite of tuffaceous pebbly graywacke and tuffaceous siltstone. Eight copper-bearing porphyry intrusions have been found in the Baogutu ore district and its surroundings and Baogutu porphyry Cu–Mo deposit occurs in the No. V pluton. Wall-rock alteration in the Baogutu deposit can be divided into four zones: the potassic alteration zone mainly includes K-feldspathization and biotitization; the main mineral assemblage of the quartz–sericite alteration zone is sericite + quartz + pyrite ± K-feldspar; the mineral assemblage of the propylitic alteration zone is chlorite + zoisite + calcite + albite ± zeolite; and the mineral assemblage of the zeolite-carbonate alteration zone is epistilbite + laumontite + calcite + quartz ± albite [17].

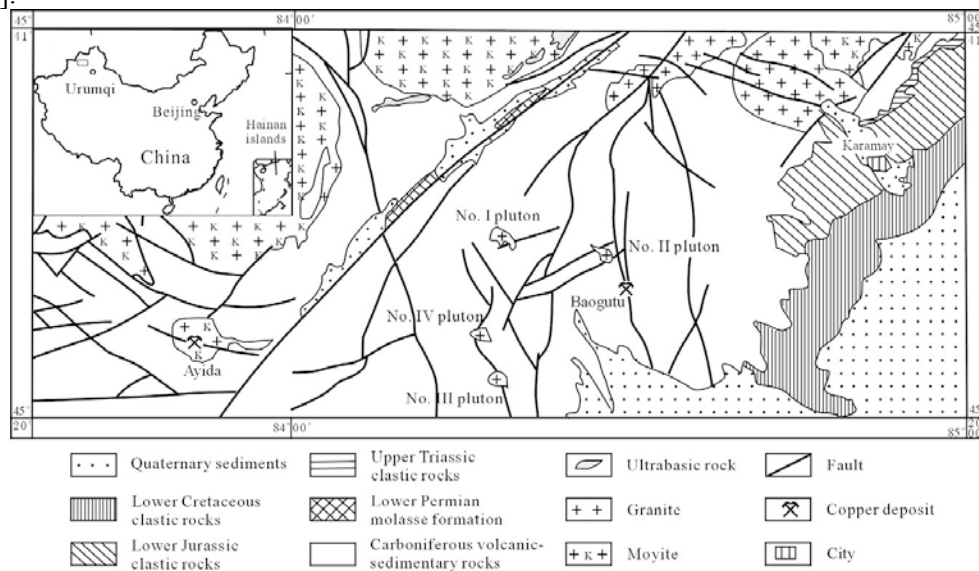


**Figure 1.** Geological map of the Baogutu porphyry copper belt (after Fuquan Yang et al.2012)

## 3. Data set and Methods

### 3.1. ASTER data

ASTER image was acquired on September 21, 2002. The image was pre-georeferenced to UTM zone 45 north projection using the WGS-84 datum. Atmospheric correction was applied by using the Fast Line-of-sight Atmospheric Analysis of Spectral Hypercubes (FLAASH) algorithm. RGB color composite of Band 3, Band2 and Band 1 is shown in figure2.

### 3.2. Image processing techniques

The performance of principal component analysis (PCA)[18], minimum noise fraction (MNF)[19] transformation and band ratio were evaluated for ASTER data to map the hydrothermally altered rocks associated with porphyry copper mineralization and lithological units. Three RBD ratios were used in this study: RBD5, RBD6, and RBD8 which were assigned for RGB (red, green, and blue) color combination to delineate argillic, phyllic and propylitic hydrothermal alteration zones [20]. Spectral mapping methods such as Constrained Energy Minimization(CEM)[21] were tested to distinguish the potassic, phyllic, argillic and propylitic alteration zones of porphyry copper mineralization using VNIR,SWIR bands of ASTER.

## 4. Results and discussion

### 4.1. The spectral feature of the alteration zones

Ideal porphyry copper deposits are typically characterized by hydrothermal alteration mineral zones. The core of quartz and potassium-bearing minerals is surrounded by multiple alteration zones[21]. The wall-rock alteration in the Baogutu deposit can be divided into four zones which is alike to the ideal porphyry copper deposits. The reflectance spectra were simulated according the mineral assemblages and their property(grain size,porosity,content et al.) by the nonlinear spectral mixture model of Hapke[23] and Shkuratov[24] using the library mineral spectra.The potassic is characterized by biotite and anhydrite with an absorption feature centered at 1.94 and 2.1 $\mu$ m. The phyllic zone is characterized by illite and sericite with an intense Al-OH absorption feature centered at 2.20 $\mu$ m, coinciding with ASTER band 6. The narrower argillic zone including kaolinite and alunite displays a secondary Al-OH absorption feature at 2.17  $\mu$ m that corresponds with ASTER band 5. The mineral assemblages of the outer propylitic zone are epidote, chlorite, and calcite that exhibit absorption features at 2.335 $\mu$ m, which coinciding with ASTER band 8 (figure 3).

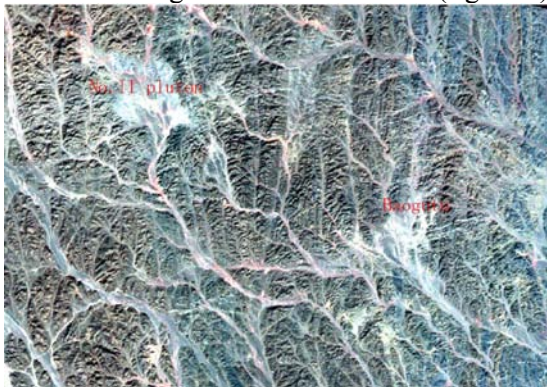


**Figure 2.** RGB color composite of Band 3, Band 2 and Band 1.

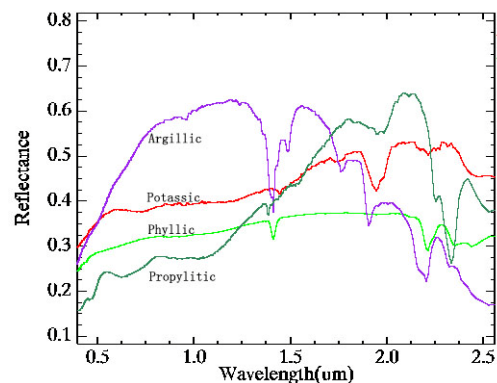


**Figure 3.** The simulated spectra of alteration mineral assemblages.

### 4.2. PCA and MNF transformation

RGB color composite image of PCA1, PCA2 and PCA3 shows plutons such as Baogutu porphyry Cu–Mo deposit as pink color (figure 4). RGB color composite of MNF eigenimages 1, 2 and 3 shows plutons as blue color areas (figure 5). Most of the rock units are all observable in the RGB color image of PCA and MNF.

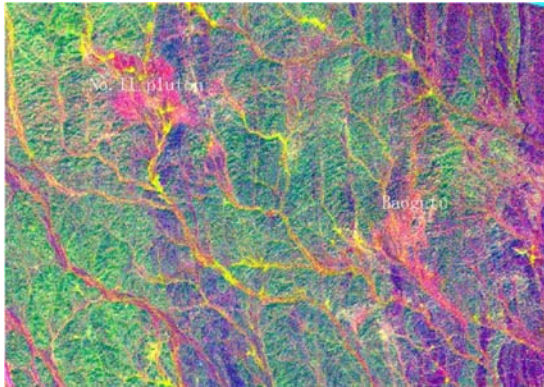


**Figure 4.** RGB color composite of PCA1, PCA2 and PCA3.

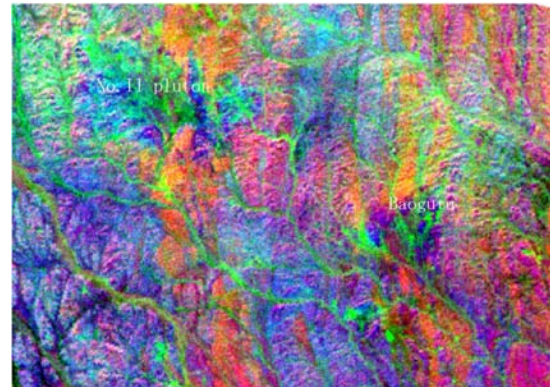


**Figure 5.** RGB color composite of MNF eginimages 1, 2 and 3.

#### 4.3. Band ratio

Relative Absorption Band Depths (RBD) consist of RBD<sub>5</sub>, RBD<sub>6</sub> and RBD<sub>8</sub> images have used in this study to delineate argillic and phyllic and propylitic mineral assemblages. RGB color composites were assigned to present the output (figure 6). Narrow argillic areas were orange color and broad phyllic was pink and yellow color that occupied major parts of the hydrothermal alteration mineral haloes, and propylitic zone as blue that surrounded outside of these hydrothermal alteration mineral zones. The location of the alteration haloes corresponded with highlighted rock units in PCA and MNF images. However, identified hydrothermal alteration zones of RBD are more recognizable than in PCA and MNF results.

#### 4.4. Mapping with CEM

Constrained Energy Minimization (CEM) method was applied to the ASTER image taking the simulated spectra of potassic, phyllic, argillic and propylitic zones as endmembers. The rule images displayed the surface distribution of hydrothermal alteration zones (figure 8-11). A circular alteration mineral zoning pattern was clearly observed in the classification result of potassic, phyllic, argillic and propylitic zones (figure 7). The results extracted by CEM technique for detecting the spatial distribution of altered zones were similar to PCA, MNF and BR results but were more detailed and precise. The distribution of four alteration zones were well alike to the field map of Shen et al., 2010. This is discernible that the spectral simulation and CEM method have a good function in identifying hydrothermally altered mineral areas than PCA, MNF and BR.

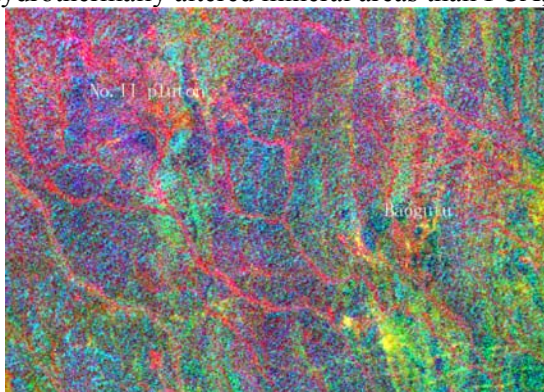


**Figure 6.** RGB color composite of RBD5, RBD6, RBD8

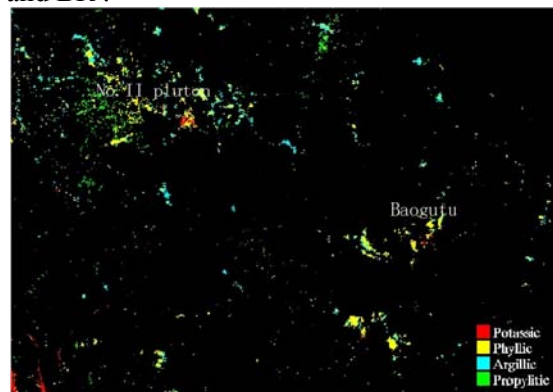


**Figure 7.** The classification result of potassic, phyllic, argillic, propylitic zones.

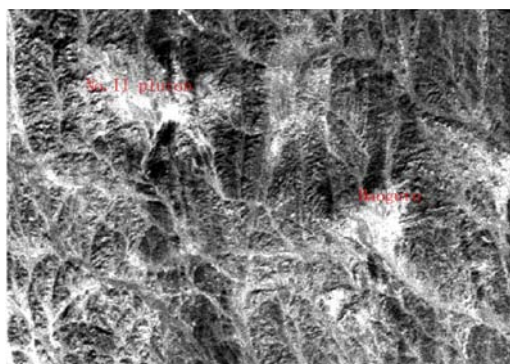


**Figure 8.** The CEM potassic rule image.

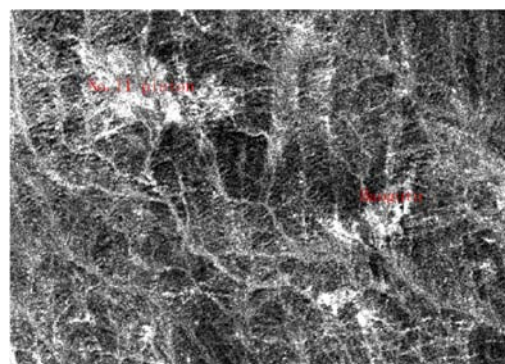


**Figure 9.** The CEM phyllic rule image

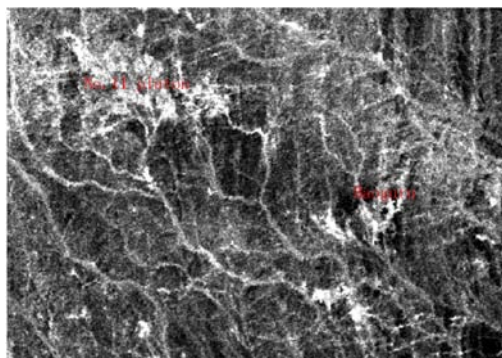


**Figure 10.** The CEM argillic rule image.

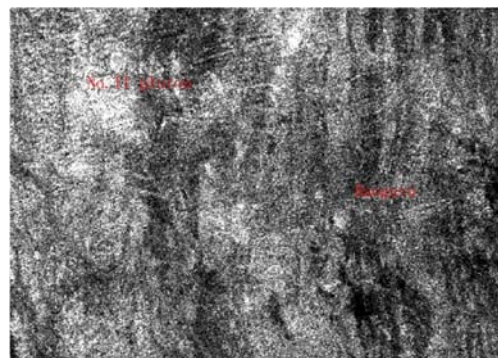


**Figure 11.** The CEM propylitic rule image

## 5. Conclusions

The study presents an approach to extract the alteration distribution information for porphyry copper exploration in the arid and semi-arid regions using ASTER image. The performance of PCA, MNF, band ratio, CEM and spectral simulation were evaluated to identify hydrothermally lithological units and alteration zones for Baogutu regions at the southern side of the Dalabute fault in the West Junggar. Spectral simulation of alteration zones and CEM methods were proved to be very suitable for distinguishing alterations as an indicator of porphyry copper mineralization zones with high economic value. Results indicate that ASTER and the integration of the image processing techniques are very effective for the mineral exploration reconnaissance stages of geologists.

## Acknowledgments

This research is supported by Natural Science Foundation of China(41102206) and The National Key Technology R&D Program(2012BAH27B05).

## References

- [1] Goetz A F H, Rock B N and Rowan, L.C. 1983 *Econ. Geol.* **78** 573–590
- [2] Sabins, F.F. 1999 *Ore Geol. Rev.* **14** 157–183
- [3] Kruse F A, Boardman J W and Huntington J F 2003 *IEEE Trans. Geosci. Remote Sens.* **41** 1388–1400
- [4] Rowan L C, Hook S J, Abrams M J and Mars J C 2003 *Econ. Geol.* **98** 1019–1027
- [5] Zhang X, Micha P and Norman D 2007 *J. Photogra. Remote Sens.* **62** 271–282
- [6] Gabr S, Ghulam A and Kusky T 2010 *Ore Geo. Rev.* **38** 59–69
- [7] Amin B P and Mazlan H 2012 *Iran Advances in Space Research* **49** 753–769
- [8] Amin B P and Mazlan H 2011 *Journal of Asian Earth Sciences* **42** 1309–1323
- [9] Hunt G R and Ashley P 1979 *Economic Geology* **74** 1613–1629
- [10] Rowan L C, Robert GS and John C 2006. *Remote Sens. Environ.* **104** 74–87

- [11] Gersman R, Ben-Dor E, Beyth M, Avigad D, Abraha M and Kibreba A 2008 *Int. J. Remote. Sens.* **29** 3911–3936
- [12] Pour B A, Hashim M and Marghany M. 2011 *International Journal of the Physical Sciences* **6** 917–929
- [13] Yamaguchi Y, Kahle A B, Kawakami T and Paniel M 1998 *IEEE Trans. Geosci. Remote Sens.* **36** 1062–1071
- [14] Hunt G R 1977 *Geophysics* **42** 501–513
- [15] Abrams M. 2000 *Int. J. Remote. Sens.* **21** 847–859
- [16] Shen P, Shen Y C, Wang J B, Zhu H P, Wang L J and Lei M. 2010 *Chem. Geol.* **275** 78–98
- [17] Yang F, Mao J, Franco P Yan S, Liu G, Zhou G, Zhang Z, Liu F, Geng X and Guo C 2012 *Journal of Asian Earth Sciences* **49** 80–98
- [18] Singh A and Harrison A 1985 *Int. J. Remote. Sens.* **6** 883–896
- [19] Green A A, Berman M, Switzer P and Craig M D 1988 *IEEE Trans. Geosci. Remote Sens.* **26** 65–74
- [20] Crowley J K, Brickey D W and Rowan L C 1989 *Remote Sens. Environ.* **29** 121–134
- [21] Harsanyi J C 1993 Detection and classification of subpixel spectral signatures in Hyperspectral image sequences (Department of Electric Engineering, University of Maryland, Baltimore County, MD)
- [22] Lowell J D and Guilbert J M 1970 *Econ. Geol.* **65** 373–408
- [23] Hapke B 1981 *J. Geophys. Res.* **86** 3039–3054
- [24] Shkuratov Y, Starukhina L, Hoffmann H, and Arnold G 1999 *Icarus* **137** 235–246